Barrel-Stave Model or Toroidal Model? A Case Study on Melittin Pores

Lin Yang, Thad A. Harroun, Thomas M. Weiss, Lai Ding, and Huey W. Huang
Department of Physics and Astronomy, Rice University Houston, Texas 77251 USA

ABSTRACT   Transmembrane pores induced by amphiphilic peptides, including melittin, are often modeled with the barrel-stave model after the alamethicin pore. We examine this assumption on melittin by using two methods, oriented circular dichroism (OCD) for detecting the orientation of melittin helix and neutron scattering for detecting transmembrane pores. OCD spectra of melittin were systematically measured. Melittin can orient either perpendicularly or parallel to a lipid bilayer, depending on the physical condition and the composition of the bilayer. Transmembrane pores were detected when the helices oriented perpendicularly to the plane of the bilayers, not when the helices oriented parallel to the bilayers. The evidence that led to the barrel-stave model for alamethicin and that to the toroidal model for magainin were reviewed. The properties of melittin pores are closely similar to that of magainin but unlike that of alamethicin. We conclude that, among naturally produced peptides that we have investigated, only alamethicin conforms to the barrel-stave model. Other peptides, including magainins, melittin and protegrins, all appear to induce transmembrane pores that conform to the toroidal model in which the lipid monolayer bends continuously through the pore so that the water core is lined by both the peptides and the lipid headgroups.

INTRODUCTION

Many naturally produced peptides, such as gene-encoded antimicrobial peptides and toxins, are known to spontaneously induce transmembrane pores in lipid bilayers under certain conditions. It is commonly believed that pore formation is the mode of action of these peptides (Boman et al., 1994); therefore, it is of importance to characterize the basic properties of this process. Until recently much of the evidence for the pore formation was either the peptide-induced ion conduction or leakage through lipid bilayers. It is difficult to determine the molecular structures of pores from such experiments. Thus, one relied on model building to help make sense of experimental observations. The first model of peptide-induced pores was proposed by Baumann and Mueller (1974) to account for the single-channel conductance induced by alamethicin in black lipid membranes. (We do not include gramicidin in this category because it forms a unique dimeric channel unlike the pores discussed here; see review by Woolley and Wallace, 1992). In this model alamethicin helices associate to form a bundle with a central lumen, like a barrel made of helical peptides as staves (Fig. 1). Ever since its introduction in the early 1970s, this barrel-stave model has been viewed as the prototype of peptide-induced transmembrane pores. Perhaps due to the lack of alternatives, peptide pores are most often described in literatures by a barrel-stave model, explicitly (e.g., Sansom, 1991) or sometimes implicitly. However, we have found and will show in this paper that, of all the

naturally produced amphiphilic peptides we have investigated, only alamethicin is consistent with the barrel-stave model.

One example that has been described as a barrel-stave model is the pore induced by melittin (Vogel and Jahnig, 1986; Sansom, 1991; Naito et al., 2000). Melittin is a cytolytic peptide extracted from bee venom (Habermann, 1972). It has been commonly used as a cell-lysing agent and is one of the most widely studied membrane-active peptides (see review by Dempsey, 1990). In this paper we will examine the pores induced by melittin in a number of different lipid bilayers, with oriented circular dichroism
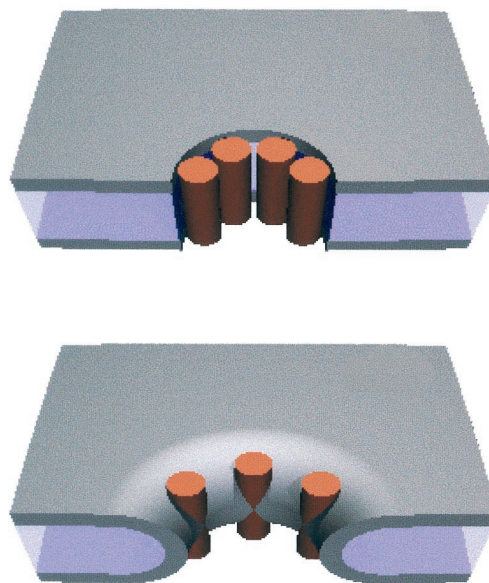
FIGURE 1   Schematics of the barrel-stave model (*top*) and the toroidal model (*bottom*). The dark layers represent the headgroup regions of bilayers. Peptide monomers are represented by the cylinders. More detailed descriptions are given in the text.

(OCD) and neutron diffraction. From these results and the experimental observations by others, we conclude that melittin pores do not conform to the barrel-stave model. Instead, they are consistent with the toroidal model that was first proposed to describe magainin-induced pores (Matsuzaki et al., 1996; Ludtke et al., 1996). The toroidal model differs from the barrel-stave model in that the peptides are always associated with the lipid headgroups even when they are perpendicularly inserted in the lipid bilayer. In forming such a pore the lipid monolayer bends continuously from the top to the bottom in the fashion of a toroidal hole, so that the pore is lined by both the peptides and the lipid headgroups (Fig. 1).

Melittin is a 26-residue linear peptide: (+)Gly-Ile-Gly-Ala-Val^5-Leu-Lys(+)-Val-Leu-Thr^{10}-Thr-Gly-Leu-Pro-Ala^{15}-Leu-Ile-Ser-Trp-Ile^{20}-Lys(+)-Arg(+)-Lys(+)-Arg(+)-Gln^{25}-Gln-NH$_2$ (Habermann and Jentsch, 1967). Its molecular structure, determined from crystals grown in aqueous solutions, is a bent α-helical rod (Eisenberg et al., 1980; Terwilliger et al., 1982). (The bending is due to the presence of a proline, a feature common among antimicrobial and toxin peptides.) Both the primary and secondary structures are similar to many antimicrobial peptides. For example, magainin 2 found in frog skin is a 23-residue linear peptide. Its NMR-deduced structure (in solutions containing >2% trifluoroethanol) is also an α-helix (Marion et al., 1988). Both peptides retain the helical conformations when bound to membranes (Vogel and Jahnig, 1986; Williams et al., 1990). In helical conformations, both peptides are strongly amphiphilic; one side along the helix largely consists of hydrophobic side chains, and the other side consists of hydrophilic side chains. Melittin has five basic side chains, and magainin has five basic and one acidic side chain, thus carrying, including the N-terminal, net +6 and +5 charges, respectively, at physiological pH. In comparison, alamethicin is a 20-residue-long, bent helix (having a Pro-14) that is also amphiphilic (Pandey et al., 1977; Fox and Richards, 1982). But it carries only one acidic side chain (Glu-18) at pH 7. Thus, alamethicin is an essentially neutral peptide that appears to be distinct from most other antimicrobial peptides which are usually highly charged. We will compare melittin with alamethicin, magainin, and a few other antimicrobial peptides in their pore-forming properties.

Antimicrobial peptides do not always form pores when they bind to membranes. In their functionally inactive state, the peptides are adsorbed in the headgroup region of lipid bilayers. Apparently, antimicrobial peptides are active, i.e., forming pores, in some cell membranes but not in others, such that they can function as host-defense agents, that is, killing invading microbes without harming self. In lipid bilayers we have found variables that can switch the peptides from the inactive to the active state or vice versa (Huang, 2000). Because different pore structures may involve different energetics, elucidation of the pore structures

is a key step toward understanding how the activities of antimicrobial peptides (and perhaps toxins) are regulated in the biological world. We have developed two different methods for detecting both the active and inactive states of peptides in oriented membranes. The method of OCD is a simple way of measuring the orientation of helical peptides in membranes (Olah and Huang, 1988; Wu et al., 1990). The method of neutron in-plane and off-plane scattering can detect and measure the sizes of transmembrane pores in membranes (He et al., 1995; Yang et al., 1998, 1999). It is important to point out that these two methods can be used to examine the same sample under identical conditions. In previous experiments on magainin and alamethicin, the pore-like diffraction patterns were observed only when the helical axes were oriented perpendicular to the plane of membranes, not when they were oriented parallel to the plane (He et al., 1995, 1996; Ludtke et al., 1996). The essential difference between the alamethicin pores and the magainin pores is in their sizes. We will review the experimental evidence that led us to conclude that the magainin pores are of the toroidal type rather than the barrel-stave type. More recently we have developed a method to observe the pore states as a function of temperature and hydration in oriented multilayer samples (Yang et al., 2000). Alamethicin and magainin behave distinctly in these experiments. Magainin pores crystallized in low hydration whereas alamethicin pores never did. We will apply all these techniques to study melittin. We will show that in most aspects melittin and magainin are similar.

MATERIALS AND METHODS

Materials

Melittin purified (85% minimum) from bee venom was purchased from Sigma Chemical Co. (St. Louis, MO). Synthetic melittin was made by Dr. James T. Sparrow (Kanda et al., 1991) using the solid-phase method as developed by Merrifield (Barany and Merrifield, 1980). 1,2-Dilauroyl-*sn*-glycero-3-phosphocholine (DLPC), 1,2-ditridecanoyl-*sn*-glycero-3-phosphocholine (DTPC), 1,2-dimyristoyl-*sn*-glycero-3-phosphocholine (DMPC), 1-palmitoyl-2-oleoyl-*sn*-glycero-3- phosphocholine (POPC), and 1,2-diphytanoyl-*sn*-glycero-3-phosphocholine (DPhPC) were purchased from Avanti Polar Lipids (Alabaster, AL). All materials were used as delivered.

Sample preparation

Two types of oriented multilayer samples were prepared. For measurements that required a rapid change in the degree of hydration, a thin film of parallel multiple bilayers of a peptide-lipid mixture was deposited on one flat substrate; we call this a one-substrate or open sample. The procedure for the preparation of a one-substrate sample was described in detail in Yang et al. (2000). Briefly, 1.5 mg of lipid and an amount of peptide corresponding to the desired peptide-to-lipid molar ratio P/L were co-dissolved in 150 μl of a mixture of 3:1 trifluoroethanol and chloroform and vortexed. The 2 $\times$ 2 cm^2 quartz plates were cleaned abrasively and soaked in a heated bath of sulfuric acid and chromic acid mixture followed by repeated washing with distilled H$_2$O and ethanol. The peptide-lipid solution was deposited onto a cleaned quartz plate and was kept undis-
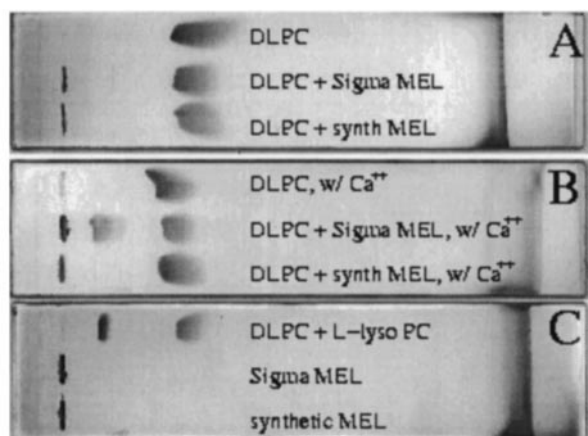
FIGURE 2 (*A*) TLC of pure DLPC, DLPC + Sigma melittin and DLPC + synthetic melittin. No lyso-PC was detected. (*B*) Ca^{2+} was added to the samples in *A*. Lyso-PC was detected in DLPC + Sigma melittin + Ca^{2+}, but not in the other two. (*C*) TLC of DLPC + lyso-PC, Sigma melittin alone, and synthetic melittin alone.

turbed during solvent evaporation. The formation of parallel multiple bilayers was proven by microscopic inspection and x-ray diffraction (Ludtke et al., 1995). For OCD measurement, one such plate was used. For neutron diffraction, six or seven plates were stacked together with spacers that kept each sample exposed to ambient air.

For neutron measurements in the fluid phase of lipids, a larger amount of sample was needed to produce a high signal-to-noise ratio. To align a larger amount of lipid bilayers, we sandwiched the sample between two substrates; we call them sandwiched samples. The procedure for preparing sandwiched samples was described in He et al. (1996). Briefly, 50 mg of lipid and an appropriate amount of peptide were co-dissolved in an organic solvent as above. After the solvent was evaporated, 2–3 ml of distilled H_2O was added to the sample, and the suspension was homogenized by a sonicator. The suspension was lyophilized until the product was fluffy and cotton-like. It was then rehydrated by D_2O vapor into a clear gel and kept fully hydrated. The sample was divided into six to seven equal portions. Each portion was aligned into parallel multi-bilayers between two consecutive quartz plates in a stack of total seven to eight plates. The sandwiched sample was then sealed in an airtight holder.

All samples for neutron diffraction used Sigma melittin. Both Sigma and synthetic melittin were used in OCD experiments.

Effect of phospholipase A_2 in Sigma melittin

Purified melittin obtained from Sigma is supposed to contain a trace amount of phospholipase A_2, which is known to hydrolyze phospholipids at the *sn*-2 position to form fatty acid and lysophospholipid products. However, the enzyme requires Ca^{2+} for activities (Gennis, 1989). We used thin layer chromatography (TLC) to detect the possible effect of phospholipase A_2 on the lipid samples containing melittin. Synthetic and Sigma melittin were each mixed with 2 mg of DLPC at P/L = 1/30 in organic solvent and dried in a bottle, exactly the same way the samples were prepared for the neutron experiment, and 0.5 ml of distilled water or 10 mM $CaCl_2$ solution was added to the bottle. The suspension was vortexed and kept in room temperature for a week. After freeze-drying, the lipid-peptide mixture was dissolved in organic solvents for TLC. The TLC assays were performed using a chloroform/methanol/water (65:25:4, v/v/v) mixture as solvent (Skipski et al., 1962). The result is shown in Fig. 2. The control runs with synthetic melittin alone, Sigma melittin alone, and DLPC + lyso-PC are shown in the Fig. 2 *C*. In Fig. 2 *B*, lyso-PC was detected in

the sample of Sigma melittin when Ca^{2+} was added, which was expected because Sigma melittin contains phospholipase A_2 as impurities. The same preparation for DLPC + synthetic melittin and another for DLPC alone, both containing Ca^{2+}, did not show lyso-PC. In Fig. 2 *A*, no lyso-PC was detected in DLPC, DLPC + Sigma melittin, or DLPC + synthetic melittin without added Ca^{2+}.

Oriented circular dichroism

OCD is a simple method for detecting the orientation of helical peptides embedded in lipid bilayers using a conventional CD machine (Olah and Huang, 1988; Wu et al., 1990). A Jasco J-500A spectropolarimeter was used for this experiment. The procedure of OCD measurement is the same as the conventional CD measurement, except that an oriented sample is used. Both types of samples described above, one-substrate and sandwiched preparations, can be used for OCD measurement. For most experiments as in this one, normal (rather than oblique) incidence OCD is sufficient for orientation analysis (Wu et al., 1990). In all cases, the results of Sigma melittin and synthetic melittin were indistinguishable. The representative results are shown in Figs. 3 and 4.

Neutron diffraction

The neutron experiment was performed at the Center for Neutron Research in the National Institute of Standards and Technology (NIST), Gaithersburg, MD, using the small-angle scattering facility NG3. The NG3 was equipped with a highly collimated neutron beam of adjustable wavelength from 0.5 to 2.0 nm and an area detector of 64×64 cm[2]. The sample-to-detector distance was adjustable from ~1 to ~13m. In addition, the detector could be moved transversely to the beam direction up to 0.3 m. The range of q (the momentum transfer) was 0.015– 6 nm^{-1}. The technique of using this facility to measure the diffraction patterns of oriented multi-lamellar membranes has been described in detail (Yang et al., 1998, 2000). Briefly, the sandwiched multilayer samples were oriented at an oblique angle with respect to the incident neutron beam so that the entire low-angle diffraction pattern was recorded by the area detector at one sample-to-detector distance, typically 2.0 m (Yang et al., 1998); this is called the off-plane scattering pattern. The sealed, sandwiched samples of melittin in DLPC, DPhPC, and POPC were measured in room temperature, so the bilayers were in the L_α (fluid) phase in all of these cases. The raw data recorded on the detector are shown in Figs. 5 and 6. The patterns were translated to the reciprocal space q_z-q_r (Fig. 5, right panels, and Fig. 7, left panels) where q_z is the momentum transfer of the neutron scattering perpendicular to the plane of bilayers and q_r the component parallel to the plane (Yang et al., 1998). Because the bilayers are two-dimensional fluids (or two-dimensional powders in the case of crystallization), there is no need for decomposing q_r into q_x and q_y.

Melittin in DTPC at P/L = 1/30 was prepared as an open sample. For this experiment, the lipid DTPC, rather than the more commonly used DLPC or DMPC, was chosen for its convenient main transition temperature, ~13.5°C. OCD measurement showed that melittin in DTPC is oriented perpendicular to the plane of membranes as in DLPC (Fig. 4) and DMPC at the same P/L (data not shown). The open sample was housed in a temperature-humidity chamber during the neutron scan as described in Yang et al. (2000). The results are shown in Fig. 8.

RESULTS

Effect of phospholipase A_2 in Sigma melittin

Apparently a trace amount of phospholipase A_2 is present in melittin obtained from Sigma. However, the effect of phospholipase A_2 is detectable only if a significant amount of
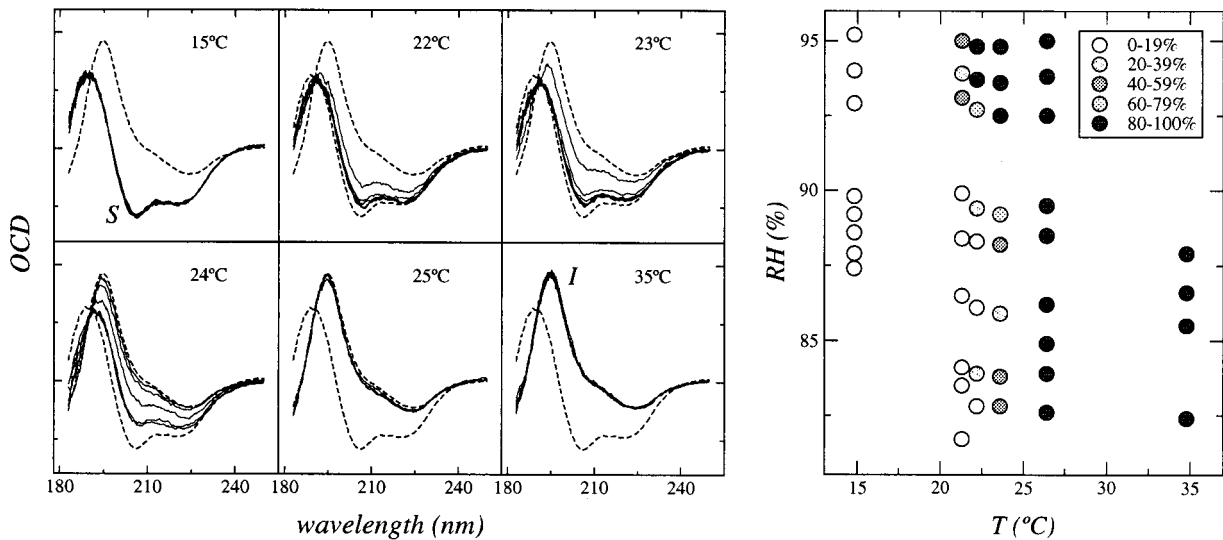
FIGURE 3 OCD spectra of one sample, melittin in DMPC at the peptide-to-lipid molar ratio P/L = 1/100, at six different temperatures and various hydration levels at each temperature (the OCD of the lipid background has been removed from each spectrum). The spectrum at 35°C (insensitive to hydration changes) is identified as the I spectrum. The spectrum at 15°C (insensitive to hydration changes) is identified as the S spectrum. I and S are shown by dashed lines in each panel as reference. Note that all other spectra fall between I and S, and each can be fit by a linear combination of I and S, from which we measured the percentage of melittin oriented parallel or perpendicular to the bilayers. The right panel shows the percentage of melittin molecules oriented perpendicularly to the bilayers in each condition.

Ca^{2+} is added to the sample. Lyso-PC was indeed detected in the lipid sample containing Sigma melittin when Ca^{2+} was added. No Ca^{2+} was added to our experimental samples and no lyso-PC was detected from them.

Both Sigma melittin and synthetic melittin were used in OCD experiments. The results of the two melittins are indistinguishable.
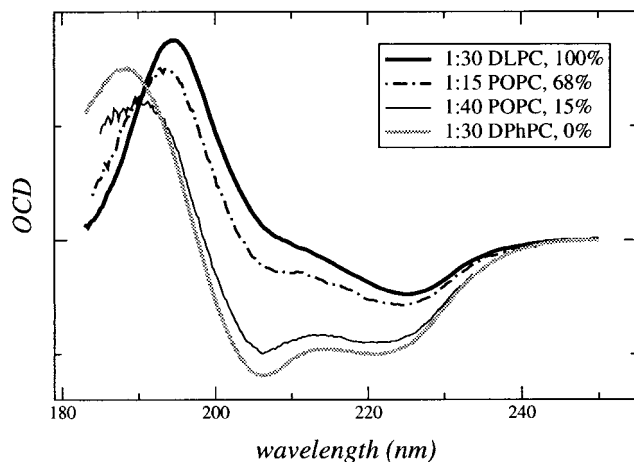

FIGURE 4 OCD spectra of four neutron samples. The spectrum of melittin in DLPC at P/L = 1/30 is the same as the I spectrum, and the spectrum of melittin in DPhPC at P/L = 1/30 is the same as the S spectrum shown in Fig. 3. The orientation of melittin in POPC depends on the peptide concentration: at P/L = 1/40 it is 85% parallel to the bilayer, and at P/L = 1/15 it is 68% perpendicular to the bilayer. The inset shows the percentage of perpendicular orientation. All were measured in room temperature and were insensitive to hydration changes.

Orientation of melittin in lipid bilayers

The OCD spectra of α-helical peptides have been discussed both experimentally and theoretically in two original papers (Olah and Huang, 1988; Wu et al., 1990). In the UV region, the spectra are dominated by the amide π-π^* and n-π^* transitions. The n-π^* transition gives rise to a negative CD band near 224 nm for helices perpendicular to the incident light (or parallel to the plane of membranes), and it decreases in magnitude and red-shifts slightly for helices parallel to the light. The π-π^* transition in a helix splits into three components: one is a negative band near 205 nm with the electric transition dipole polarized parallel to the helical axis so this component is absent for helices parallel to the light, and the other two have their electric transition dipoles polarized perpendicular to the helical axis and give rise to a positive Gaussian band centered near 190 nm when the helix is normal to the light. When the helix is parallel to the light, the positive band has a shape of the negative derivative of a Gaussian and is red shifted relative to the normal-to-light band. These spectra vary somewhat from one helical peptide to another, probably because none of them are perfect α-helices for the entire length (Okada et al., 1994). In general, if one measures the OCD of a peptide in a number of different lipids as a function of P/L, temperature, and hydration, particularly if the variety of the lipid includes both saturated and unsaturated chains, the normal- and parallel-to-light spectra will appear as two extreme spectra (Huang and Wu, 1991; Ludtke et al., 1994; Heller et al., 1998). And if the peptide can exist only in two orientations,
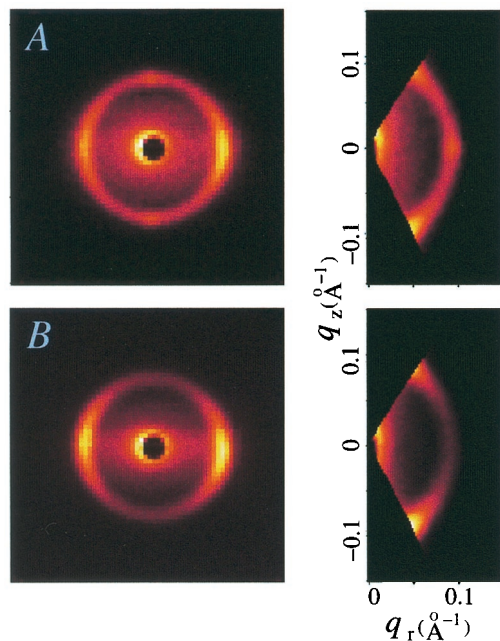
FIGURE 5 Neutron off-plane scattering of melittin in DPhPC at P/L = 1/30 (A) and melittin in POPC at P/L = 1/40 (B). The multilamellar samples were oriented at 60° with respect to the incident neutron beam (see Yang et al., 1998). The left panel shows the raw data recorded on the area detector. The data were translated to the reciprocal space q_z-q_r on the right panel. The circular arcs are due to smectic defects in the samples. Similar patterns were obtained from pure lipid samples (He et al., 1996).

all other spectra are linear superpositions of the two. The two extreme spectra of melittin were found in DMPC bilayers at P/L = 1/100 in high and low temperatures (Fig. 3). According to the spectral theory qualitatively described above, melittin is oriented parallel to the light, or perpendicular to the bilayer, in the spectrum labeled I and oriented perpendicular to the light, or parallel to the bilayer, in the spectrum labeled S. All other OCD spectra can each be fit by a linear combination of I and S, from which one measures the percentage of the peptide oriented either parallel or
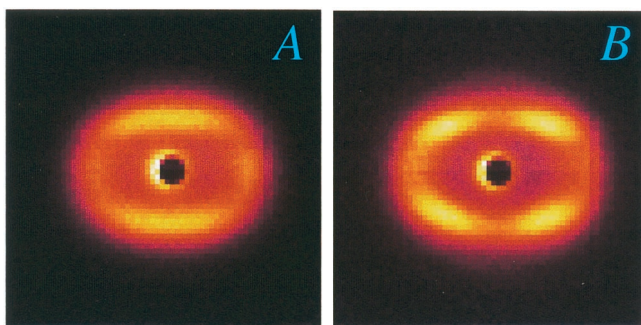

FIGURE 6 Neutron off-plane scattering of melittin in POPC at P/L = 1/15 (A) and melittin in DLPC at P/L = 1/30 (B), measured in the same manner as the two samples in Fig. 5, recorded on the area detector. The signals are dominated by the diffraction patterns of transmembrane pores.

perpendicular to the bilayers. The diagram on the right panel of Fig. 3 shows how the orientation of melittin changes with temperature and hydration. It appears that, in the case of DMPC, melittin is inserted perpendicularly in fluid bilayers but oriented parallel to the bilayer in the gel phase. This, however, is not a general rule for other lipids (see below).

Fig. 4 shows the OCD of the four samples that were used for neutron experiments. The spectra show that melittin in DLPC at P/L = 1/30 is perpendicular to the plane of the bilayers. Melittin in DPhPC at P/L = 1/30 is parallel to the plane of the bilayers. Melittin in POPC at P/L = 1/40 is 85% parallel to the bilayer but at P/L = 1/15 is 68% perpendicular to the bilayer. The decompositions to the normal and parallel components were obtained by fitting each spectrum with a linear superposition of the I and S spectra. The lipid bilayers of these four samples were in the fluid phase, and the spectra were insensitive to hydration change.

Analysis of neutron diffraction

The two samples, melittin in DPhPC at P/L = 1/30 and melittin in POPC at P/L = 1/40, for which the OCD has shown that melittin is primarily oriented parallel to the plane of membranes are shown in Fig. 5, as the control. Each pattern is essentially a circular arc with a radius corresponding to $q = 2\pi/d$ where d is the lamellar repeat spacing. If the samples were perfectly oriented multi-bilayers, the circular arcs should be absent. The arcs were due to the presence of smectic defects called oily streaks in the samples, as described in detail in He et al. (1996). These patterns are the same as that produced by a pure lipid sample with defects. There are no in-plane structures in these bilayers. In contrast, diffraction patterns (Fig. 6) characteristically different from Fig. 5 were recorded for melittin in DLPC at P/L = 1/30 and melittin in POPC at P/L = 1/15, for which OCD has shown that melittin is primarily oriented perpendicular to the plane of membranes. These are the typical diffraction patterns of transmembrane pores in fluid membranes, because neutron was mainly scattered by D_2O penetrating the lipid bilayers. The analyses of these patterns have been discussed recently in Yang et al. (1999).

In Fig. 7 A, *right*, the q_z dependence of the diffraction peak is compared with that of the form factor of a cylinder of height equivalent to the bilayer thickness, representing the D_2O column inside the pore (see details in Yang et al., 1999). When the q_z dependence of the diffraction pattern is that of the form factor of a pore, it implies that the individual pores are positionally uncorrelated from one bilayer to the other bilayers. The q_r dependence of the diffraction pattern (Fig. 7 A, *middle*) is governed by the theory of scattering from a two-dimensional fluid (Yang et al., 1999):

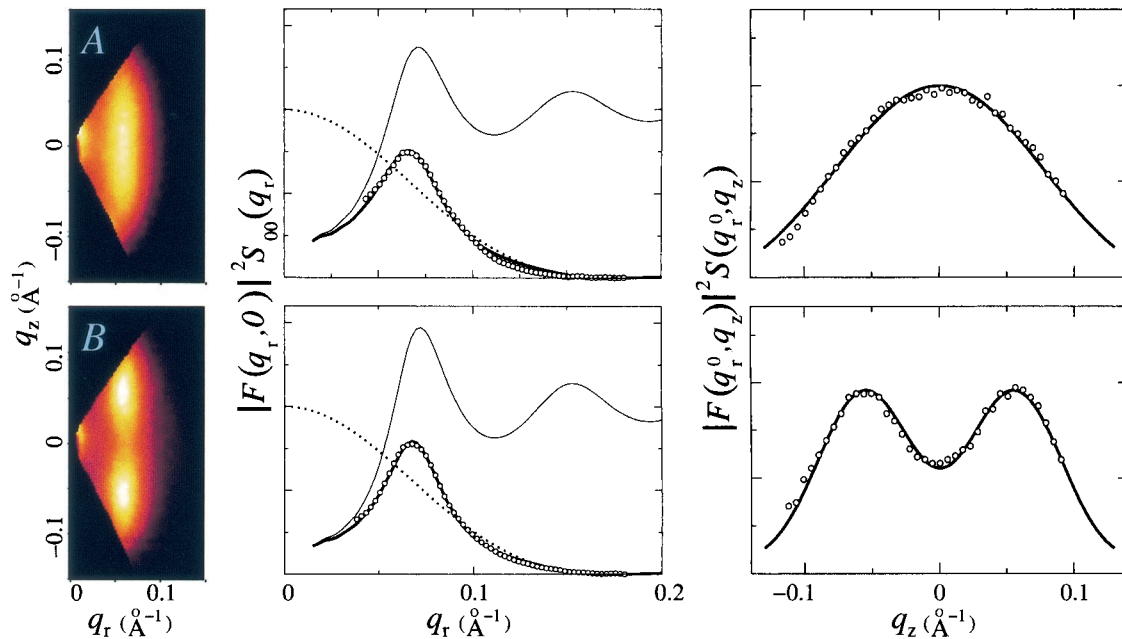$$I_{00}(0, q_r) = |F_\phi(0, q_r)|^2 S_{00}(q_r), \qquad (1)$$

FIGURE 7 (A, left) The data on Fig. 6 A were translated to the reciprocal space q_z-q_r. (A, middle) The circles are the data points along q_r at $q_z = 0$. The dotted line is $|F_\phi(0, q_r)|^2$ of a cylinder representing the D_2O pore, essentially determined by one parameter representing the diameter. The thin solid line is $S_{00}(q_r)$ computer-simulated by freely diffusing hard disks, essentially determined by the disk concentration and the disk size. The latter represents the contact distance between two pores or the outside diameter of the pores. The thick solid line is the fit to the data by $|F_\phi(0, q_r)|^2 S_{00}(q_r)$. (A, right) The circles are the data points along q_z at $q_r = q_r^o = 0.066$ Å^{-1} (the q_r position of the peak). The solid line is the q_z dependence of the form factor $|F_\phi(q_z, q_r)|^2$ of a cylinder of height 33 Å. (B, left) The data on Fig. 6 B were translated to the q_z-q_r plane. (B, middle) The circles are the $|F_\phi(0, q_r)|^2 S_{00}(q_r)$ component obtained from the data on the left. The fit to the data was similar to A. (B, right) The circles are the data points from the left panel along q_z at $q_r = q_r^o = 0.068$ Å^{-1}, the q_r position of the peaks. The solid line is the q_z dependence of $a_1|F_\phi(q_z, q_r)|^2[1 + a_2\cos(q_z d)]$ (see Eq. 2) with the form factor $|F_\phi(q_z, q_r)|^2$ of a cylinder of height 30 Å and the repeat spacing $d = 45$ Å. a_1 and a_2 are constants.

where the scattering intensity $I_{00}(0, q_r)$ has been normalized to one pore (Warren, 1969) and the subscript 00 indicates that the density correlations (that give rise to the scattering) are within one individual bilayer. The form factor $F_\phi(q_z, q_r) = F_p(q_z, q_r) - F_{lb}(q_z, q_r)$ is the form factor of the pore $F_p(q_z, q_r)$ minus the form factor of a patch of lipid bilayer $F_{lb}(q_z, q_r)$ filling the space of the pore (see Yang et

al., 1999), and $S_{00}(q_r)$ is the partial structure factor within an individual bilayer.

The diffraction pattern of melittin in DLPC (Fig. 6 B) looks very different from that of melittin in POPC (Fig. 6 A). This is because in this DLPC sample, at the condition of measurement, the in-plane positions of the pores are correlated between neighboring bilayers. As explained in two
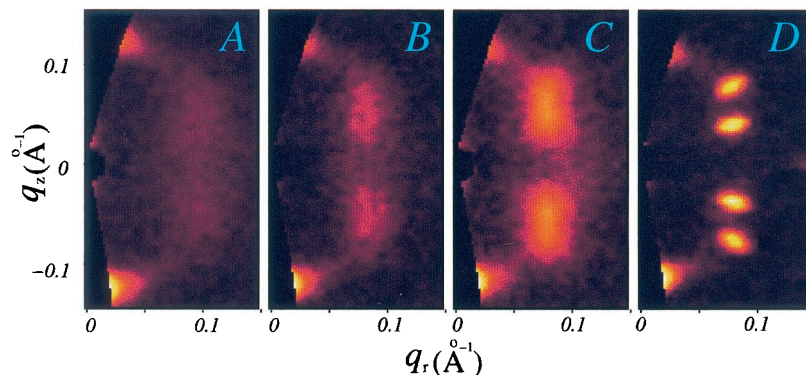

FIGURE 8 Neutron diffraction patterns of one sample, melittin in DTPC at P/L = 1/30, housed in a temperature-humidity chamber. Inside the chamber, the open sample was exposed to air of controlled D_2O humidity. (A) 27°C, 99% RH; (B) 20°C, 95% RH; (C) 17°C, 98% RH; (D) 10°C, 94% RH. The changes were reversible and reproducible.

previous papers (Yang et al., 1999, 2000), such correlations occur (due to the hydration force between bilayers) when the sample is less than fully hydrated. In this case the scattering intensity $I(q_z, q_r)$ is given by (Yang et al., 1999)

$$I(q_z, q_r) = |F_\phi(q_z, q_r)|^2 S(q_z, q_r) \qquad (2.1)$$

$$S(q_z, q_r) = S_{00}(q_r) + 2\cos(q_z d)S_{01}(q_r) + \ldots, \quad (2.2)$$

where $S_{01}(q_r)$ is the partial structure factor between the nearest neighboring bilayers. In principle, there is a partial structure factor between a bilayer and its next nearest neighboring bilayers and so forth, but so far we have been able to analyze the data with two terms shown in Eq. 2.2. Fig. 7 B, $right$, shows that the q_z dependence of the diffraction pattern is described by a form given by Eq. 2.2. As was shown in our previous analysis (Yang et al., 1999), it is possible to make use of the factor $\cos(q_z d)$ in Eq. 2.2 to separate the S_{00} term and the S_{01} term from the diffraction pattern. Fig. 7 B, $middle$, shows the $I_{00}(0, q_r) = |F_\phi(0, q_r)|^2 S_{00}(q_r)$ term obtained from the diffraction pattern shown in the left panel. In our previous experiments with magainins and protegrins, we found that the pore size (and hence I_{00}) varied with lipid (Yang et al., 1999; 2000). But here $I_{00}(0, q_r)$ of the melittin pores in POPC is very close to the corresponding $I_{00}(0, q_r) = |F_\phi(0, q_r)|^2 S_{00}(q_r)$ of the melittin pores in DLPC. In both cases, the form factor $F_\phi(0, q_r)$ is essentially that of the D_2O cylinder inside the pore. The function $F_\phi(0, q_r)$ is essentially determined by the diameter of the D_2O cylinder or the inside diameter of the pore. The structure factor $S_{00}(q_r)$ was computer-simulated by freely diffusing hard disks of an undetermined diameter that corresponds to the contact distance between two pores, or the effective outside diameter of the pore (He et al., 1996). Thus the data fitting (Fig. 7, $middle$) produces the estimates for the inside and outside diameters of the pores (see the detailed data analyses in He et al., 1996; Yang et al., 1999). The pores in POPC have an inside diameter of 4.4 nm and an outside diameter of 7.6 nm. The pores in DLPC are similar, 4.4 nm and 7.8 nm.

More detailed model fittings are possible. For example, in previous papers we have considered the form factor based on an assumed model (Ludtke et al., 1996) and the effect of hydrogen-deuterium exchange on peptides (He et al., 1996). The results were not significantly different from the simple model as presented above. We believe that the 4.4-nm-diameter for the water pore does not disagree with the estimates by vesicle leakage experiments (Katsu et al., 1988; Ladokhin et al., 1997; Matsuzaki et al., 1997). They all reported pore size up to a diameter of ~3 nm that apparently was increasing with melittin concentration. On the other hand, in our experiments (He et al., 1996; Ludtke et al., 1996) the pore size was quite independent of peptide concentration (for P/L $\geq$ 1/30). It is not clear what value of peptide concentration in the leakage experiment should be compared with ours. We also note that leakage experiments tend to underestimate the pore size.

Crystallization of melittin pores

Fig. 8 shows a series of diffraction patterns indicating different degrees of correlation between bilayers: from having negligible correlation in a close to fully hydrated condition (Fig. 8 A) to having long-ranged correlation (i.e., crystallization) in a condition of low temperature and low humidity (Fig. 8 D). These phenomena of correlations between bilayers and crystallization of peptide organizations in lipid bilayers have been observed previously in magainin and protegrin samples (Yang et al., 2000) but never occurred in alamethicin samples. This seems to indicate that the pores induced by magainin, protegrin, and melittin are structurally different from the pores induced by alamethicin.

DISCUSSION

The orientation of melittin in lipid bilayers has been a controversial issue (e.g., Okada et al., 1994; Naito et al., 2000), in part, at least in the past, due to an implicit assumption made by some investigators that a helical peptide must bind to a lipid bilayer with a definite orientation. However, over the years it has been gradually realized that the orientation of a membrane-bound helical peptide can vary with the physico-chemical condition of the bilayer (Vogel et al., 1983; Vogel, 1987; Brauner et al., 1987; Altenbach et al., 1989; Frey and Tamm, 1991). In particular, the simplicity of the OCD method has allowed us to investigate numerous peptide-lipid combinations in many different conditions (Olah and Huang, 1988; Wu et al., 1990; Huang and Wu, 1991; Ludtke et al., 1994; Heller et al., 1997, 1998). We have found that one of the most important controlling variables for the orientation is the peptide concentration. In general, at a given level of hydration and temperature, a helical peptide is bound parallel to a lipid bilayer when the concentration P/L is below a certain threshold value P/L*. As P/L increases above P/L*, an increasing fraction of the peptide molecules change to the perpendicular orientation, until above another threshold concentration, all of the peptide molecules become oriented perpendicularly. This threshold concentration for insertion P/L* varies greatly with both peptide and lipid. Because samples of very high P/L ($>$1/10) are difficult to prepare and, on the other hand, peptide signal is undetectable for very low P/L ($<$1/300), a given peptide-lipid combination often reveals only one orientation within the detectable range of P/L. Other important variables for the orientation include the sample hydration and temperature. Again, the sensitivity of these variables varies with peptide and lipid. For example, melittin appears to be oriented perpendicular to the DLPC, DTPC, and DMPC bilayers for all the P/L

values ($>1/120$) we have experimented, if the temperature is well above their respective gel-to-fluid transition point. On the contrary, in the same range of P/L, melittin is always oriented parallel to the DPhPC bilayers, with little dependence on temperature and hydration. To produce unambiguous signal from neutron experiment, we needed a lipid bilayer in which melittin would change orientation above P/L of ~1/40. This was found in POPC. As shown in Fig. 4, melittin is 85% parallel to the bilayers at P/L = 1/40 and is 68% perpendicular to the bilayers at P/L = 1/15.

In DMPC bilayers, we showed how the orientation of melittin varies with temperature and hydration (Fig. 3). One might be tempted to conclude from the DMPC example that melittin is inserted perpendicularly in fluid bilayers but adsorbs parallel to the surface of gel-phase bilayers, but this is not a general rule. Melittin appears not to insert in DPhPC bilayers, which are fluid unless severely dehydrated (Hung et al., 2000). And in POPC, another fluid bilayer, melittin can orient either parallel or perpendicularly to the plane of the membrane depending on the peptide concentration. Taken together with similar observations on alamethicin (Huang and Wu, 1991; Heller et al., 1997) and magainin (Ludtke et al., 1994), it is clear that the orientation of a helical peptide is a function of the physical condition and the chemical composition of the lipid bilayer. Theoretically, only some aspects of the principles that determine the orientation of a peptide are understood. For example, if the membrane-thinning effect (Wu et al., 1995; Ludtke et al., 1995; Heller et al., 2000) is the mechanism for the peptide orientation change, one can understand how it depends on the areal ratio of the lipid headgroup to its chains (Heller et al., 1997).

OCD measurement of melittin orientation is consistent with previous measurements by other techniques mentioned above when the same lipid systems were used. In particular, our measurement is consistent with the temperature-induced change of orientation in DMPC reported by Vogel (1987) and the hydration dependence reported by Frey and Tamm (1991). More recently, Naito et al. (2000) used magnetically oriented vesicles to investigate the orientation of melittin by solid-state NMR. Melittin was found to insert transmembrane in DMPC bilayers in the fluid phase at P/L ≈ 1/10 (consistent with the OCD measurement above).

Neutron is uniquely capable of detecting water penetrating through lipid bilayers because of the strong contrast in the neutron-scattering length density between D_2O and lipid (He et al., 1996). Neutron diffraction clearly showed that melittin-induced transmembrane pores were present when and only when the peptide was primarily oriented perpendicular to the bilayers. No pores were detected when OCD showed that the peptide was primarily oriented parallel to the bilayers. The same is true with alamethicin (He et al., 1996) and magainin (Ludtke et al., 1996). There should not be any more doubt that transmembrane pores are formed by helical peptides oriented perpendicular to the plane of bi-layers. This is not to say that only helical peptides are capable of pore formation. Indeed, transmembrane pores induced by β-sheet peptide protegrin-1 have also been observed by the same technique (Yang et al., 2000).

To assess the possible structure of the melittin pore, it is useful to review briefly the evidence that led to the barrel-stave model for alamethicin and the toroidal model for magainin. The most important evidence for the barrel-stave model is the single-channel conductance induced by alamethicin that is characterized by reproducible multiple discrete states (Baumann and Mueller, 1974; Latorre and Alvarez, 1981; Mak and Webb, 1995). This behavior of ion conduction naturally suggested the barrel-stave model in which the channel changes its conductance state when a single alamethicin molecule joins or leaves the aggregate. The model also explained the dependence of the channel activity on voltage (Hall et al., 1984) and on membrane tension (Opsahl and Webb, 1994). Neutron scattering showed that alamethicin pores in DLPC have an inside diameter of ~1.8 nm and an outside diameter of ~4.0 nm (He et al., 1996). These dimensions imply that the wall of the channel is ~1.1 nm in thickness, and this is the same as the diameter of the alamethicin helix according to the crystal structures of alamethicin helices (Fox and Richards, 1982). Thus, the neutron-determined dimensions of alamethicin pores are entirely consistent with the barrel-stave model composed of eight alamethicin monomers (He et al., 1996).

Ion conductance induced by magainin did not show multiple discrete levels as in the case of alamethicin. In fact, the conductance level of magainin varied from one experiment to another (Duclohier et al., 1989). This is very different from alamethicin for which different laboratories have reproduced the same conductance levels using the same lipid systems (Mak and Webb, 1995). Thus, the structure of the magainin pores appears to be continuously variable rather than discrete. There is no reason to invoke a barrel-stave model to describe the magainin pores based on the single-channel conductance experiments. Neutron scattering showed that the magainin pores are substantially larger and with a greater size variation compared with the alamethicin pores (Ludtke et al., 1996; Yang et al., 1999). In a number of different lipid bilayers, their inside diameters are 3.0–5.0 nm with corresponding outside diameters of 7.0–8.4 nm. These dimensions are not consistent with the barrel-stave model for several reasons. First, crystallographic analyses (Terwilliger et al., 1982) and monolayer studies (DeGrado et al., 1981) both gave a cross-sectional area along the melittin helix close to 4.00 nm^2, implying that the diameter of the melittin helix is ~1.0–1.1 nm. The crystallographic analysis by Terwilliger et al. (1982) had taken into account the solvent content of the crystals, whereas the alamethicin diameter of 1.1 nm might be slightly overestimated because it was not corrected for the solvent content in the alamethicin crystals (~30% solvent; Fox and Richards, 1982). These

results are consistent with each other, because melittin side chains (average MW 109 per amino acid) are somewhat bulkier than alamethicin side chains (average MW 98 per amino acid). Thus, it is reasonable to assume that 1.0–1.1 nm is the typical size for helical peptides, including magainin (average MW 107 per amino acid). This dimension is substantially smaller than the walls of the channels measured above 1.7–2.0 nm. Second, from the density of the pores in the membrane measured by neutron scattering and the percentage of perpendicularly oriented peptides by OCD, we estimated only four to seven magainin monomers in each pore (Ludtke et al., 1996). These numbers of monomers are insufficient to form a barrel-stave model comparable to the diameters measured. Third, the sizes of the pores also disfavor the barrel-stave model from the viewpoint of mechanics. A barrel-stave model with a water pore greater than 3.0 nm in diameter would consist of a bundle of 12 or more peptide helices, which is most likely unstable against shape deformation and is outside the observed range of 5–10 peptides reported in alamethicin experiments (Mak and Webb, 1995). These difficulties are resolved by the toroidal model in which the lipid monolayer continuously bends from the top leaflet to the bottom leaflet through a toroidal hole, so the pore is lined by both the lipid headgroups and peptide helices. The helices are embedded among the lipid headgroups as in the case of surface adsorption and are oriented perpendicular to the plane of the bilayer according to the OCD result given above. The dimensions of the toroidal model are expected to be continuously variable depending on P/L and the physical properties of the lipid bilayer, such as the elasticity constants, which in turn depend on the degree of hydration, temperature, etc. Unlike the barrel-stave model, the toroidal model should be mechanically stable against shape deformation even in a large size (manuscript in preparation). This model was proposed by us for the magainin pores because of their physical dimensions determined by neutron diffraction and for an important constraint that magainin has been observed to be always associated with the lipid headgroups rather than with the lipid chains (Ludtke et al., 1996). This constraint was found by a wide range of experiments, including Raman (Williams et al., 1990), fluorescence (Matsuzaki et al., 1994), differential scanning calorimetry (Matsuzaki et al., 1991), and NMR (Hirsh et al., 1996). An equivalent model was independently proposed by Matsuzaki's group (Matsuzaki et al., 1996) based on their innovative fluorescence and leakage experiments and in part to account for the observed lipid flip-flop during the leakage. However, we note that lipid flip-flop was also observed during alamethicin-induced conduction (Hall, 1981).

Another important distinction between magainin and alamethicin is in what happens when the pores are subjected to hydration and temperature changes. For magainin in high P/L (1/50–1/15), once the pores were formed in fluid lipid bilayers, such peptide-lipid supramolecular structures crystallized when the samples were dehydrated and/or cooled (Yang et al., 2000). But under the same conditions, alamethicin pores never crystallized. These experiments have been repeated many times, and the results so far have been the same. This is a strong indication that the molecular configurations of magainin pores and alamethicin pores are different, further justifying two different models for these two pores.

The argument for the two models above is based on experimental evidence. Another argument can be made by considering the effects of the charges carried by the peptides. A magainin monomer may carry as many as +5 charges at physiological pH. The fact that the pores are formed by approximately seven monomers in each pore implies that these charges are effectively screened; otherwise the Coulomb energy would be so high that pore formation would not be possible (Bechinger, 1997). Besides ions, water molecules and lipid headgroups are effective in screening due to their large polarizability (Debye, 1929; Hasted, 1973; Israelachvili, 1992). We believe that in the toroidal model the lipid headgroups play an important role in screening the peptide charges, whereas such screening would be absent in the barrel-stave model. This could be the reason why only an essentially neutral peptide like alamethicin seems to form barrel-stave pores. (We note that multilayer samples are not ion-free. The concentration of counter-ions in water would be as high as ~0.3 M if five polar side chains were ionized in each peptide at P/L = 1/30.)

Very few ion conduction experiments with melittin have been published, as far as we know. Early experiments by Tosteson and Tosteson (1981) reported discrete levels of conductance somewhat similar to alamethicin. However, the data of more recent experiments showed single-channel conductance similar to magainin (Hanke et al., 1983; Sansom, 1991). Various studies on the location of melittin within the bilayer were also inconclusive (for reviews see Dempsey, 1990; Sansom, 1991). Thus, our conclusion is drawn mainly from our neutron experiment. Both the inside and outside diameters, 4.2 and 7.7 nm, of melittin pores are comparable to that of magainin (Yang et al., 1999) in DLPC bilayers. The pores crystallized in the same manner as magainin pores when the sample was dehydrated and cooled. These properties agree with the toroidal model but not with the barrel-stave model. The experimental data of other peptides we have investigated including magainin analogs, protegrin-1 and protegrin analogs (see Yang et al., 1998, 1999, 2000) also conform to the toroidal model. So far, among naturally produced peptides, only alamethicin has been found to be describable by the barrel-stave model.

In recent years there has been increasing interest in membrane-active antimicrobial peptides (e.g., Ganz, 1999, 2000; Martin et al., 1995). Gene-encoded peptide antibiotics are ubiquitous components of host defenses in mammals, birds, amphibians, insects, and plants. Extensive evidence showed

that these small proteins (20–40 residues in length) act by permeabilizing the cell membranes of microorganisms (see reviews in Boman et al., 1994; Shai, 1999). Interestingly, melittin has similar molecular characteristics as antimicrobial peptides, and its action on cell membranes is also similar (Tossi et al., 2000). The difference is that melittin is antibacterial as well as hemolytic, whereas the host-defense peptides are antibacterial but non-hemolytic (Oren and Shai, 1997). It is therefore of great interest from the points of view of fundamental principles and of potential pharmaceutical applications to understand the similarities and differences between melittin and antimicrobial peptides

REFERENCES

Altenbach, C. W. Francisz, J. S. Hyde, and W. L. Hubbell. 1989. Conformation of spin-labeled melittin at membrane surfaces investigated by pulse saturation recovery and continuous wave power saturation electron paramagnetic resonance. *Biophys. J.* 56:1183–1191.

Barany, G., and R. B. Merrifield. 1980. Solid phase synthesis. *In* The Peptides: Analysis, Synthesis, Biology. E. Gross and J. Meienhofer, editors. Academic Press, New York. 3–284.

Baumann, G., and P. Mueller. 1974. A molecular model of membrane excitability. *J. Supramol. Struct.* 2:538–557.

Bechinger, B. 1997. Structure and functions of channel-forming peptides: magainins, cecropins, melittin and alamethicin. *J. Membr. Biol.* 156: 197–211.

Boman, H. G., J. Marsh and J. A. Goode. 1994. Antimicrobial peptides. *Ciba Found. Symp.* 186:1–272.

Brauner, J. W., R. Mendelsohn, and F. G. Prendergast. 1987. Attenuated total reflectance Fourier transform infrared studies of the interaction of melittin, two fragments of melittin and d-hemolysin with phosphatidylcholines. *Biochemistry.* 26:8151–8158.

Debye, P. 1929. Polar Molecules. Chemical Catalog Co., New York. 109–124.

DeGrado, W. F., F. J. Kezdy, and E. T. Kaiser. 1981. Design, synthesis and characterization of a cytotoxic peptide with melittin-like activity. *J. Am. Chem. Soc.* 103:679–681.

Dempsey, C. E. 1990. The actions of melittin on membranes. *Biochim. Biophys. Acta.* 1031:143–161.

Duclohier, H., G. Molle, and G. Spach. 1989. Antimicrobial peptide magainin 1 from *Xenopus* skin forms anion-permeable channels in planar lipid bilayers. *Biophys. J.* 56:1017–1021.

Eisenberg, D., T. C. Terwilliger, and F. Tsui. 1980. Structural studies of bee melittin. *Biophys. J.* 32:252–254.

Fox, R. O., and F. M. Richards. 1982. A voltage-gated ion channel model inferred from the crystal structure of alamethicin at 1.5-Å resolution. *Nature.* 300:325–330.

Frey, S., and L. K. Tamm. 1991. Orientation of melittin in phospholipid bilayers. *Biophys. J.* 60:922–930.

Gennis, R. B. 1989. Biomembranes. Springer-Verlag, New York. 231–234.

Ganz, T. 1999. Defensins and host defense. *Science.* 286:420–421.

Ganz, T. 2000. Paneth cells: guardians of the gut cell hatchery. *Nat. Immunol.* 2:99–100.

Habermann, E. 1972. Bee and wasp venom: the biochemistry and pharmacology of their peptides and enzymes are reviewed. *Science.* 177: 314–322.

Habermann, E., and J. Jentsch. 1967. Sequenzanalyse des Melittins aus den tryptischen und peptischen Spaltstucken. *Hope-Seylers Z. Physiol. Chem.* 348:37–50.

Hall, J. E. 1981. Voltage-dependent lipid flip-flop induced by alamethicin. *Biophys. J.* 33:373–381.

Hall, J. E., I. Vodyanov, T. M. Balasubramanian, and G. R. Marshall. 1984. Alamethicin: a rich model for channel behavior. *Biophys. J.* 45:233–247.

Hanke, W., C. Methfessel, H.-U. Wilmsen, E. Katz, G. Jung, and G. Boheim. 1983. Melittin and a chemically modified trichotoxin form alamethicin-type multi-state pores. *Biochim. Biophys. Acta.* 727: 108–114.

Hasted, J. B. 1973. Aqueous Dielectrics. Chapman and Hall, London. 136–174.

He, K., S. J. Ludtke, D. L. Worcester, and H. W. Huang. 1995. Antimicrobial peptide pores in membranes detected by neutron in-plane scattering. *Biochemistry.* 34:15614–15618.

He, K., S. J. Ludtke, D. L. Worcester, and H. W. Huang. 1996. Neutron scattering in the plane of membranes: structure of alamethicin pores. *Biophys. J.* 70:2659–2666.

Heller, W. T., K. He, S. J. Ludtke, T. A. Harroun, and H. W. Huang. 1997. Effect of changing the size of lipid headgroup on peptide insertion into membranes. *Biophys. J.* 73:239–244.

Heller, W. T., A. J. Waring, R. I. Lehrer, T. A. Harroun, T. M. Weiss, L. Yang, and H. W. Huang. 2000. Membrane thinning effect of the β-sheet antimicrobial protegrin. *Biochemistry.* 39:139–145.

Heller, W. T., A. J. Waring, R. I. Lehrer, and H. W. Huang. 1998. Multiple states of b-sheet peptide protegrin in lipid bilayers. *Biochemistry.* 37: 17331–17338.

Hirsh, D. J., J. Hammer, W. L. Maloy, J. Blazyk, and J. Schaefer. 1996. Secondary structure and location of a magainin analogue in synthetic phospholipid bilayers. *Biochemistry.* 35:12733–12741.

Huang, H. W. 2000. Action of antimicrobial peptides: two-state model. *Biochemistry.* 39:8347–8352.

Huang, H. W., and Y. Wu. 1991. Lipid-alamethicin interactions influence alamethicin orientation. *Biophys. J.* 60:1079–1087.

Hung, W. C., F. Y. Chen, and Huey W. Huang. 2000. Order-disorder transition in bilayers of diphytanoyl phosphatidylcholine. *Biochim. Biophys. Acta.* 1467:198–206.

Israelachvili, J. 1992. Intermolecular and Surface Forces. Academic Press, New York. 37, 199, 237–256.

Kanda, P. R. C. Kennedy, and J. T. Sparrow. 1991. Synthesis of polyamide supports for use in peptide synthesis and as peptide-resin conjugates for antibody production. *Int. J. Peptide Protein.* 38:385–391.

Katsu, T. C. Ninomiya, M. Kuroko, H. Kobayashi, T. Hirota, and Y. Fujita. 1988. Action mechanism of amphipathic peptides gramicidin S and melittin on erythrocyte membrane. *Biochim. Biophys. Acta.* 939:57–63.

Ladokhin, A. S., M. E. Selsted, and S. H. White. 1997. Sizing membrane pores in lipid vesicles by leakage of co-encapsulated markers: pore formation by melittin. *Biophys. J.* 72:1762–1766.

Latorre, R., and O. Alvarez. 1981. Voltage-dependent channels in planar lipid bilayer membranes. *Physiol. Rev.* 61:77–150.

Ludtke, S. J., K. He, W. T. Heller, T. A. Harroun, L. Yang, and H. W. Huang. 1996. Membrane pores induced by magainin. *Biochemistry.* 35:13723–13728.

Ludtke, S., K. He, and H. W. Huang. 1995. Membrane thinning caused by magainin 2. *Biochemistry.* 34:16764–16769.

Ludtke, S. J., K. He, Y. Wu, and H. W. Huang. 1994. Cooperative membrane insertion of magainin correlated with its cytolytic activity. *Biochim. Biophys. Acta.* 1190:181–184.

Mak, D. D., and W. W. Webb. 1995. Two classes of alamethicin transmembrane channels: molecular models form single-channel properties. *Biophys. J.* 69:2323–2336.

Marion, D., M. Zasloff, and A. Bax. 1988. A two-dimensional NMR study of the antimicrobial peptide magainin 2. *FEBS Lett.* 227:21–26.

Martin, E., T. Ganz, and R. I. Lehrer. 1995. Defensins and other endogenous peptide antibiotics of vertebrates. *J. Leukocyte Biol.* 58:128–136.

Matsuzaki, K., M. Harada, S. Fumakoshi, N. Fujii, and K. Miyajima. 1991. Physicochemical determinants for the interactions of magainins 1 and 2 with acidic lipid bilayers. *Biochim. Biophys. Acta.* 1063:162–170.

Matsuzaki, K., O. Murase, H. Tokuda, N. Fujii, and K. Miyajima. 1996. An antimicrobial peptide, magainin 2, induced rapid flip-flop of phospholipids coupled with pore formation and peptide translocation. *Biochemistry.* 35:11361–11368.

Matsuzaki, K., O. Murase, H. Tokuda, S. Fumakoshi, N. Fujii, N., and K. Miyajima. 1994. Orientational and aggregational states of magainin 2 in phospholipid bilayers. *Biochemistry.* 33:3342–3349.

Matsuzaki, K., S. Yoneyama, and K. Miyajima. 1997. Pore formation and translocation of melittin. *Biophys. J.* 73:831–838.

Naito, A., T. Nagao, K. Norisada, T. Mizuno, S. Tuzi, and H. Saito. 2000. Conformation and dynamics of melittin bound to magnetically oriented lipid bilayers by solid state ^{31}P and ^{13}C NMR spectroscopy. *Biophys. J.* 78:2405–2417.

Okada, A., K. Wakamatsu, T. Miyazawa, and T. Higashijima. 1994. Vesicle-bound conformation of melittin: transferred nuclear Overhauser enhancement analysis in the presence of perdeuterated phosphatidylcholine vesicles. *Biochemistry.* 33:9438–9446.

Olah, G. A., and H. W. Huang. 1988. Circular dichroism of oriented α-helices. I. Proof of the exciton theory. *J. Chem. Phys.* 89:2531–2538.

Opsahl, L. R., and W. W. Webb. 1994. Transduction of membrane tension by the ion channel alamethicin. *Biophys. J.* 66:71–74.

Oren, Z., and Y. Shai. 1997. Selective lysis of bacteria but not mammalian cells by diastereomers of melittin: structure-function study. *Biochemistry.* 36:1826–1835.

Pandey, R. C., J. C. Cook, and K. L. Rinehart. 1977. High resolution and field desorption mass spectrometry studies and revised structure of alamethicin I and II. *J. Am. Chem. Soc.* 99:8469–8483.

Sansom, M. P. 1991. The biophysics of peptide models of ion channels. *Prog. Biophys. Mol. Biol.* 55:139–215.

Shai, Y. 1999. Mechanism of the binding, insertion and destabilization of phospholipid bilayer membranes by α-helical antimicrobial and cell non-selective membrane-lytic peptides. *Biochim. Biophys. Acta.* 1462:55–70.

Skipski, V. P., R. F. Peterson, and M. Barclay. 1962. Separation of phosphatidyl ethanolamine, phosphatidyl serine, and other phospholipids by thin layer chromatography. *J. Lipid Res.* 3:467–470.

Terwilliger, T. C., L. Weissman, and D. Eisenberg. 1982. The structure of melittin in the form I crystals and its implication for melittin's lytic and surface activities. *Biophys. J.* 37:353–361.

Tossi, A., L. Sandri, and A. Giangaspero. 2000. Amphipathic, α-helical antimicrobial peptides. *Biopolymers.* 55:4–30.

Tosteson, M. T., and D. C. Tosteson. 1981. The sting: melittin forms channels in lipid bilayers. *Biophys. J.* 36:109–116.

Vogel, H. 1987. Comparison of the conformation and orientation of alamethicin and melittin in lipid membranes. *Biochemistry.* 26:4552–4572.

Vogel, H., and F. Jahnig. 1986. The structure of melittin in membranes. *Biophys. J.* 50:573–582.

Vogel, H., F. Jahning, V. Hoffman, and J. Stumpel. 1983. The orientation of melittin in lipid membranes. A polarized infrared spectroscopic study. *Biochim. Biophys. Acta.* 733:201–209.

Warren, B. E. 1969. X-ray Diffraction. Dover, New York. 125.

Williams, R. W., R. Starman, K. M. P. Taylor, K. Cable, T. Beeler, M. Zasloff, and D. Covell. 1990. Raman spectroscopy of synthetic antimicrobial frog peptides magainin 2a and PGLa. *Biochemistry.* 29:4490–4496.

Woolley, G. A., and B. A. Wallace. 1992. Model ion channels: gramicidin and alamethicin. *J. Membr. Biol.* 129:109–136.

Wu, Y., K. He, S. J. Ludtke, and H. W. Huang. 1995. X-ray diffraction study of lipid bilayer membrane interacting with amphiphilic helical peptides: diphytanoyl phosphatidylcholine with alamethicin at low concentrations. *Biophys. J.* 68:2361–2369.

Wu, Y., H. W. Huang, and G. A. Olah. 1990. Method of oriented circular dichroism *Biophys. J.* 57:797–806.

Yang, L., T. A. Harroun, W. T. Heller, T. M. Weiss, and H. W. Huang. 1998. Neutron off-plane scattering of aligned membranes. I. Method of measurement. *Biophys. J.* 75:641–645.

Yang, L., T. M. Weiss, T. A. Harroun, W. T. Heller, and H. W. Huang. 1999. Supramolecular structures of peptide assemblies in membranes by neutron off-plane scattering: method of analysis. *Biophys. J.* 77:2648–2656.

Yang, L., T. M. Weiss, R. I. Lehrer, and H. W. Huang. 2000. Crystallization of antimicrobial pores in membranes: magainin and protegrin. *Biophys. J.* 79:2002–2009.